



Double grating systems with one steel tape grating

Francisco Jose Torcal-Milla*, Luis Miguel Sanchez-Brea, Eusebio Bernabeu

Universidad Complutense de Madrid, Applied Optics Complutense Group, Optics Department, Facultad de Ciencias Físicas, Ciudad Universitaria s.n., 28040 Madrid, Spain

ARTICLE INFO

Article history:

Received 5 February 2008

Received in revised form 27 June 2008

Accepted 11 August 2008

PACS:

42.25._p

42.25.Fx

42.25.Hz

42.79.Dj

ABSTRACT

Steel tape gratings are used in different metrology applications. As the period of these gratings was large (around 100 μm), its analytical study has been performed, up to date, using a geometrical approach. Nowadays, steel tape gratings can be manufactured with lower periods, around 20–40 μm , and diffractive effects must be taken into account. Also, due to the roughness of the surface, statistical techniques need to be considered to analyze their behavior. In this work, an analysis of the pseudo-imaging formation in a double grating system including one steel tape grating is performed. In particular Moiré and Lau configurations are analyzed. We have found that roughness significantly affects to Moiré configuration. However, its effect is negligible in Lau configuration. Generalized grating imaging configuration is also studied in depth. It is shown that roughness does not affect to the contrast of pseudoimages, but it modifies their depth of focus.

© 2008 Elsevier B.V. All rights reserved.

1. Introduction

Double grating systems are used in numerous applications such as metrology, interferometry [1–3], and spectrometry [4,5], existing several common configurations [6,7]. In Moiré configuration, a plane wave illuminates a system formed by two gratings of the same period [8]. Then fringes are observed just after the second grating. The well-known Talbot effect appears, that is, a periodic modulation of contrast in terms of the distance between gratings. The period of this modulation is the well-known Talbot distance $z_T = p^2/\lambda$, where p is the period of the gratings and λ the wavelength. In so-called Lau configuration, on the other hand, a point source is not required. [9,10]. The observation plane is located at infinite and, in practice, a lens is used to detect fringes at its focal plane [11]. In Generalized Grating Imaging configuration the two gratings may present equal or different periods and fringes are obtained at finite distances from the second grating [12–15]. As a consequence, the devices which use this configuration are more compact and robust, since no lenses are required.

In most applications, chrome on glass gratings are used. They are easily manufactured and their period can be very small. However, glass gratings are not appropriate for measuring displacements longer than 3 m, since they are difficult to manufacture and handle. In these cases, steel tape gratings are used. This kind of gratings can be much more easily manufactured for longer lengths than chrome on glass gratings. Besides, their handling is not critical. However, some disadvantages appear. The period of

steel tape gratings is larger. Traditionally, the standard periods for steel tape gratings were around 100 μm , and a geometrical analysis was enough to determine the main characteristics of the fringes. Nowadays, periods of 20–40 μm are available for commercial steel tape gratings [16]. With this range of periods, the diffractive behavior of the gratings must be taken into account. Also, steel tape gratings are not ideal, because their surface presents a certain roughness due to the fabrication process and to the nature of the substrate. This roughness produces adverse effects in the self-imaging process [17,18].

In this work, we analyze double grating systems when one of the gratings is a steel tape grating. In particular, we have analyzed the fringe formation when the first grating is a steel tape grating and the second grating is an amplitude grating (for example, a chrome on glass grating). A scalar Fresnel approach is used for the propagation calculations since the period of the gratings is much larger than the wavelength of the light used. Also, owing to the rough surface, statistical techniques need to be used to determine the average intensity distribution at the observation plane. The case where the first grating is an amplitude grating and the second grating is a steel tape grating can be easily derived from this work.

2. Theoretical approach

The general configuration for a double grating system is shown in Fig. 1a, where the first grating is a steel tape grating and the second one is an amplitude grating (chrome on glass grating). Let us consider a monochromatic light source with wavelength λ and lateral size S . The periods of the gratings, p_1 and p_2 , respectively, are assumed much larger than the wavelength and then a scalar

* Corresponding author.

E-mail address: ftorcalmilla@fis.ucm.es (F.J. Torcal-Milla).

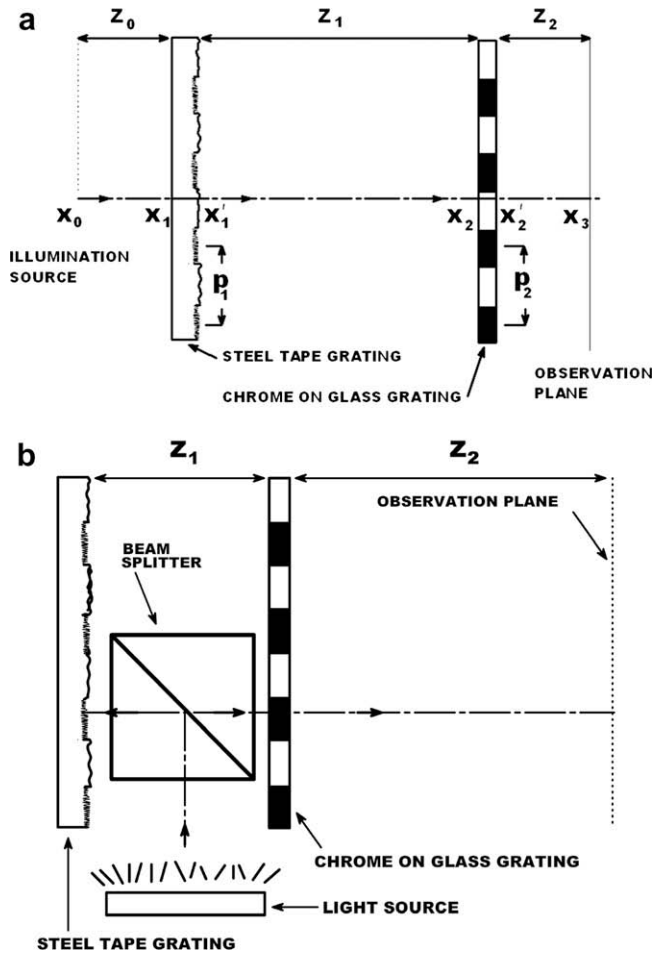


Fig. 1. (a) Standard set-up for a double grating system showing the parameters involved. (b) Set-up when a steel tape grating is used. Since the first grating is opaque, a beam splitter is required for the illumination.

approach is acceptable. As shown in Fig. 1, the distances between the source, gratings, and observation plane are, respectively, denoted by z_0 , z_1 , and z_2 . Since the system is symmetrical along the y -axis, a 2-D analysis can be performed. The steel tape grating is opaque and then the configuration depicted in Fig. 1a is only valid for theoretical purposes. On the other hand, a practical set-up is shown in Fig. 1b where a beam splitter is used to illuminate the grating. This set-up can be used to analyze all the double grating configurations. The light source is made up of point-like emitters which incoherently generate divergent spherical waves. By the moment, let us consider one of these point emitters placed at a distance x_0 from the axis. The amplitude just before the first grating is given by the Fresnel propagation of a single point source

$$U_1(x_1, z_0) = \frac{A_0}{\sqrt{i\lambda z_0}} \exp\left[\frac{ik}{2z_0}(x_1 - x_0)^2\right], \quad (1)$$

A_0 being the amplitude, $k = 2\pi/\lambda$, and x_1 the transversal coordinate at the first grating plane. Light is reflected by the first grating (steel tape grating). As it is shown in [17], the steel tape grating presents two roughness levels. The high roughness level scatters light in all directions and its contribution to the diffraction pattern is a constant background intensity. Then, the reflectance of the steel tape grating can be mathematically described as the product of two terms $T(x_1) = g_1(x_1)t(x_1)$. The first term is a binary amplitude grating whose infinite Fourier series is $g_1(x_1) = \sum_n a_n \exp(inq_1 x_1)$, where $q_1 = 2\pi/p_1$, and a_n is the n th coefficient of the grating with n integer.

The second term, $t(x_1)$, includes the topography of the rough surface. It is defined using a stochastic function, $\zeta(x_1)$, whose average height is zero $\langle \zeta(x_1) \rangle = 0$. Taking the thin element approach, the reflectance due to roughness is given by $t(x_1) = \exp[-2ik\zeta(x_1)]$, [19,20]. Then, the amplitude of the light field after the grating results

$$\hat{U}(x_1, z_0) = \frac{A_0}{\sqrt{i\lambda z_0}} \exp\left[\frac{ik}{2z_0}(x_1 - x_0)^2\right] t(x_1) \sum_n a_n \exp(inq_1 x_1). \quad (2)$$

The next step is to propagate the field up to the second grating, placed at a distance z_1 from the first grating

$$U(x_2, z_1) = \frac{A_0}{i\lambda\sqrt{z_0 z_1}} \int_{-\infty}^{\infty} \sum_n a_n \exp(inq_1 x_1) \exp\left[\frac{ik}{2z_0}(x_1 - x_0)^2\right] t(x_1) \times \exp\left[\frac{ik}{2z_1}(x_2 - x_1)^2\right] dx_1. \quad (3)$$

The second grating is a binary amplitude grating with period p_2 which is also described by its Fourier Series expansion $g_2(x_2) = \sum_m b_m \exp(imq_2 x_2)$, where b_m is the m th coefficient of the grating with m integer, $q_2 = 2\pi/p_2$, and x_2 is the transversal coordinate at the second grating plane. Thus, the amplitude of the light field after the second grating is given by

$$\hat{U}(x_2, z_1) = g_2(x_2) U(x_2, z_1) = \frac{A_0}{i\lambda\sqrt{z_0 z_1}} \int_{-\infty}^{\infty} \sum_n a_n \exp(inq_1 x_1) \sum_m b_m \exp(imq_2 x_2) \times \exp\left[\frac{ik}{2z_0}(x_1 - x_0)^2\right] t(x_1) \times \exp\left[\frac{ik}{2z_1}(x_2 - x_1)^2\right] dx_1. \quad (4)$$

Finally, light propagates along a distance z_2 from the second grating up to the location of the photodetector or the observation plane and the amplitude is

$$U(x_3, z_2) = \frac{A_0}{(i\lambda)^{3/2} \sqrt{z_0 z_1 z_2}} \int_{-\infty}^{\infty} \int_{-\infty}^{\infty} \sum_n a_n \exp(inq_1 x_1) \times \sum_m b_m \exp(imq_2 x_2) \exp\left[\frac{ik}{2z_0}(x_1 - x_0)^2\right] t(x_1) \times \exp\left[\frac{ik}{2z_1}(x_2 - x_1)^2\right] \exp\left[\frac{ik}{2z_2}(x_3 - x_2)^2\right] dx_1 dx_2. \quad (5)$$

An exact equation for the field at the observation plane cannot be determined since the topography $\zeta(x_1)$ is stochastic and thus the reflectance coefficient $t(x_1)$ is unknown. Nevertheless, the average intensity at the observation plane (x_3, z_2) can be calculated from the amplitude using an averaging process, $\langle I(x_3, z_2) \rangle = \langle U(x_3, z_2) U^*(x_3, z_2) \rangle$, where $\langle \bullet \rangle$ represents the average over a hypothetical ensemble of rough surfaces. We will assume that roughness is stationary and, therefore, the amplitude correlation of the speckle field is stationary too. The only stochastic factor in the intensity equation is $\langle t(x_1) t^*(x_1') \rangle$, which is known as the autocorrelation function of the surface [19]. In many theoretical and experimental works on roughness a Gaussian function is used to represent the autocorrelation function $\langle t(x_1) t^*(x_1') \rangle = \exp[-(x_1 - x_1')^2 / T_0^2]$, T_0 being the correlation length of the field. The correlation length of the field is related to the roughness parameters according to $T_0 = \lambda T / 4\pi\sigma$, where T is the correlation length of the roughness and σ is the standard deviation in heights [21]. After a straightforward calculation, the average intensity at the observation plane results

$$\begin{aligned}
 \langle I(x_3, z_2) \rangle &= \frac{A_0^2}{\lambda z_T} \sum_{n, n', m, m' = -\infty}^{\infty} a_n a_n^* b_m b_m^* \\
 &\times \exp \left\{ - \left[z_0 \frac{(n - n') q_1 z_{12} + (m - m') q_2 z_2}{k T_0 z_T} \right]^2 \right\} \\
 &\times \exp \left\{ -i \left[(n^2 - n'^2) \frac{q_1^2 z_0 z_{12}}{2k z_T} + (m^2 - m'^2) \frac{q_2^2 z_2 z_{01}}{2k z_T} \right] \right\} \\
 &\times \exp \left\{ -i \left[(n' - n) q_1 \frac{(x_3 z_0 + x_0 z_{12})}{z_T} + (m' - m) q_2 \frac{(x_3 z_{01} + x_0 z_2)}{z_T} \right] \right\} \\
 &\times \exp \left\{ -i \left[(mn - m'n') \frac{q_1 q_2 z_0 z_2}{k z_T} \right] \right\}, \quad (6)
 \end{aligned}$$

being $z_T = z_0 + z_1 + z_2$, $z_{12} = z_1 + z_2$, and $z_{01} = z_0 + z_1$. The effect of roughness appears in the first Gaussian term of (6) and produces a decreasing of the average intensity at the observation plane. This reduction depends on the correlation length of the field T_0 , the distances involved, the periods of the gratings, and the wavelength of the incident beam. From this general approach, some important cases can be analyzed, such as Moiré, Lau or Generalized Grating Imaging configurations.

2.1. Moiré configuration

Moiré effect can be derived from Eq. (6) considering that both gratings have the same period $p_1 = p_2 = p$ and placing the light source at infinite, $z_0 \rightarrow \infty$. Then, the mean intensity for Moiré configuration results

$$\begin{aligned}
 \langle I(x_3) \rangle &\propto \sum_{n, n', m, m' = -\infty}^{\infty} a_n a_n^* b_m b_m^* \\
 &\times \exp \left\{ - \left[q \frac{(n - n') z_{12} + (m - m') z_2}{k T_0} \right]^2 \right\} \\
 &\times \exp \left\{ -i \frac{q^2}{2k} [(n^2 - n'^2) z_{12} + (m^2 - m'^2) z_2] \right\} \\
 &\times \exp \{ i q x_3 [(n - n') + (m - m')] \} \\
 &\times \exp \left[-i \frac{q^2}{k} (mn - m'n') z_2 \right]. \quad (7)
 \end{aligned}$$

Classically, Moiré effect is analyzed when the observation plane coincides with the second grating plane, $z_2 \rightarrow 0$. Thus, Eq. (7) simplifies to

$$\begin{aligned}
 \langle I(x_3) \rangle &\propto \sum_{n, n', m, m' = -\infty}^{\infty} a_n a_n^* b_m b_m^* \\
 &\times \exp \left\{ - \left[q \frac{(n - n') z_1}{k T_0} \right]^2 \right\} \\
 &\times \exp \left\{ -i \frac{q^2}{2k} [(n^2 - n'^2) z_1] \right\} \\
 &\times \exp \{ i q x_3 [(n - n') + (m - m')] \}. \quad (8)
 \end{aligned}$$

In Moiré configuration, the presence of roughness produces a Gaussian decreasing of the intensity in terms of z_1 , which is shown in Fig. 2. The relative displacement Δx between gratings can be included in the equations using the following change: $a_n \rightarrow a_n \exp(iq n \Delta x)$. Then the average intensity distribution results

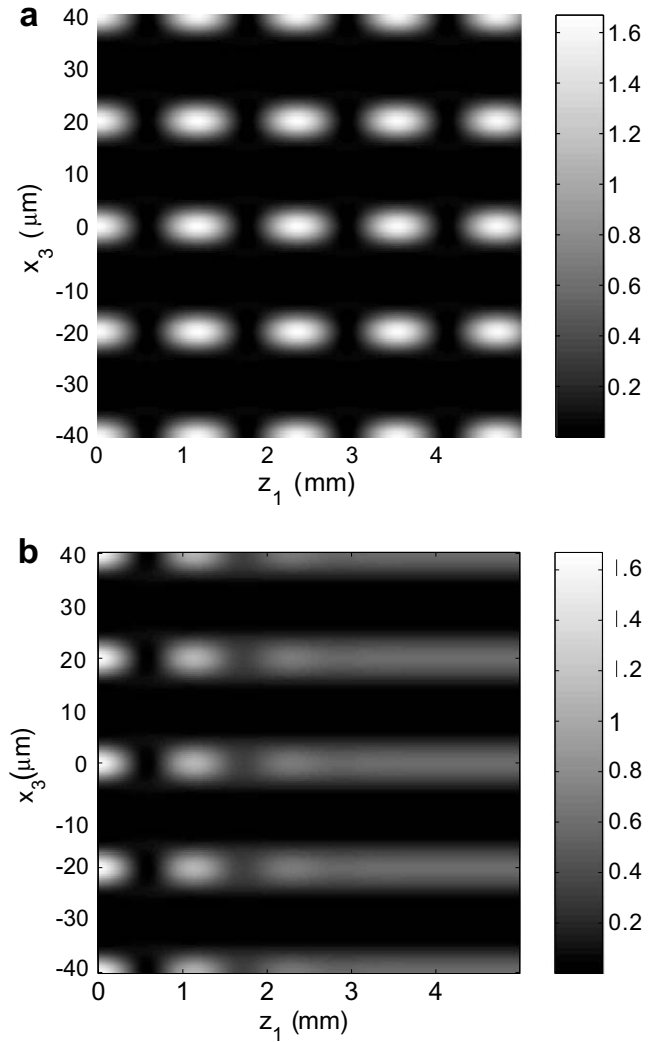


Fig. 2. Fringes obtained with a Moiré configuration when the wavelength is $\lambda = 0.68 \mu\text{m}$ and the period of both gratings is $p = 20 \mu\text{m}$. (a) The first grating is a chrome on glass grating. (b) The first grating is a steel tape grating whose roughness parameters are $\sigma = 0.1 \mu\text{m}$, $T = 50 \mu\text{m}$.

$$\begin{aligned}
 \langle I(x_3) \rangle_M &\propto \sum_{n, n', m, m' = -\infty}^{\infty} a_n a_n^* b_m b_m^* \exp [i q (n - n') \Delta x] \\
 &\times \exp \left\{ - \left[q \frac{(n - n') z_1}{k T_0} \right]^2 \right\} \exp \left\{ -i \frac{q^2}{2k} [(n^2 - n'^2) z_1] \right\} \\
 &\times \exp \{ i q x_3 [(n - n') + (m - m')] \}. \quad (9)
 \end{aligned}$$

When $z_1 \gg k T_0 / q$, the only significant terms are those that fulfill $n = n'$. Then the information about the relative displacement between gratings disappears and the second grating receives a constant field. On the other hand, when roughness is zero, $T_0 \rightarrow \infty$, the classical expression of Moiré effect is recovered.

2.2. Lau configuration

Lau effect can also be obtained from Eq. (6) considering that the size of the source is infinite, $S \rightarrow \infty$, assuming $p_1 = p_2 = p$, and placing the observation plane at infinite, $z_2 \rightarrow \infty$. We will consider first a source of finite size S and perform an integration in x_0 with the following limits: $-S/2 < x_0 < S/2$. Then the average intensity is

$$\begin{aligned}
\langle I(\theta) \rangle \propto & \sum_{n,n',m,m'=-\infty}^{\infty} a_n a_n^* b_m b_m^* \\
& \times \exp \left\{ - \left[\frac{z_0 q}{k T_0} (n - n' + m - m') \right]^2 \right\} \exp \left[-i \frac{q^2}{2k} (n^2 - n'^2) z_0 \right] \\
& \times \exp \left[-i \frac{q^2}{2k} (m^2 - m'^2) z_{01} \right] \exp \{ i q \theta [(n - n') z_0 + (m - m') z_{01}] \} \\
& \times \exp \left[-i \frac{q^2}{k} (m n + m' n') z_0 \right] \operatorname{sinc} \left[\frac{q S}{2} (n - n' + m - m') \right],
\end{aligned} \quad (10)$$

where we have used $\theta = x_3/z_2$ and $\operatorname{sinc}(x) = \sin(x)/x$. For an infinite source we need to consider the limit $S \rightarrow \infty$, and then the sinc function tends to a Kronecker delta function $\delta(n - n' + m - m')$. Thus, the average intensity simplifies to

$$\begin{aligned}
\langle I(\theta) \rangle_I \propto & \sum_{n,n',m,m'=-\infty}^{\infty} a_n a_n^* b_{(-n+n'+m')} b_{m'}^* \\
& \times \exp \left[-i \frac{q^2}{2k} (n - n')^2 z_1 \right] \exp \left[-i \frac{q^2}{k} (n' - n) m' z_1 \right] \\
& \times \exp [-i q \theta (n - n') z_1].
\end{aligned} \quad (11)$$

Roughness dependence disappears from the equation and the expression obtained corresponds to the classical expression for the Lau effect [22].

2.3. Generalized grating imaging

Generalized grating imaging configuration has become very common because, for it, lenses are not required to obtain fringes. Due to this, this kind of devices is more compact and robust. The period of the gratings can be equal or different and the light source has finite size, S . Fringes are formed at finite distances from the second grating. The expression for generalized grating imaging when a finite source is considered can be determined from Eq. (6). The light source can be considered as a sum of incoherent point sources. Then the average intensity can be obtained as an integration of Eq. (6) between $-S/2 < x_0 < S/2$, resulting in

$$\begin{aligned}
\langle I(x_3, z_2) \rangle \propto & \sum_{n,n',m,m'=-\infty}^{\infty} a_n a_n^* b_m b_m^* \\
& \times \exp \left(- \left\{ \frac{z_0}{k T_0 z_T} [(n - n') q_1 z_{12} + (m - m') q_2 z_2] \right\}^2 \right) \\
& \times \exp \left\{ -i \frac{1}{2k z_T} [(n^2 - n'^2) q_1^2 z_0 z_{12} + (m^2 - m'^2) q_2^2 z_2 z_{01}] \right\} \\
& \times \exp \left\{ - \frac{i x_3}{z_T} [(n' - n) q_1 z_0 + (m' - m) q_2 z_{01}] \right\} \\
& \times \exp \left\{ -i \left[(m n - m' n') \frac{q_1 q_2 z_0 z_2}{k z_T} \right] \right\} \\
& \times \operatorname{sinc} \left\{ \frac{S}{2 z_T} [(n - n') q_1 z_{12} + (m - m') q_2 z_2] \right\}.
\end{aligned} \quad (12)$$

The intensity distribution depends on the correlation length of the field T_0 , as it is shown in Fig. 3. When the distance between the light source and the first grating z_0 is zero, the exponential term associated to roughness disappears and (12) becomes the standard equation for the generalized grating imaging phenomenon with finite source [14]. When the light source is infinite ($S \rightarrow \infty$), the sinc function tends to a Kronecker delta function $\delta[(n - n') q_1 z_{12} + (m - m') q_2 z_2]$. In this case, the roughness effect also disappears for any distance z_0 and the mean intensity is given by

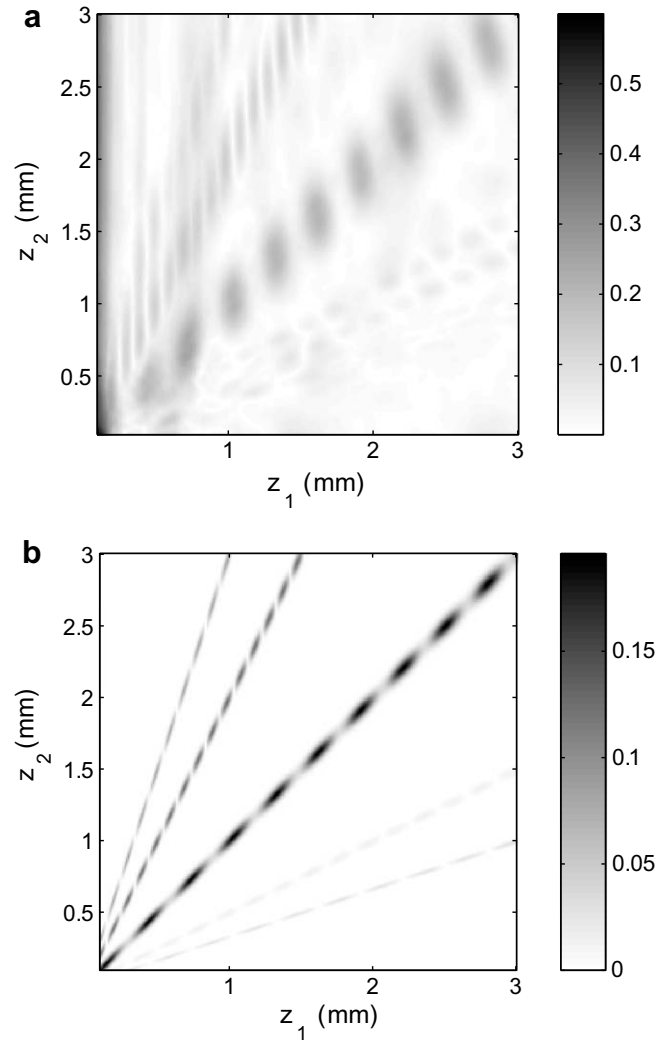


Fig. 3. Self-images obtained in generalized grating imaging (a) without considering roughness, (b) considering roughness, $\sigma = 0.5 \mu\text{m}$, $T = 10 \mu\text{m}$. In both cases the wavelength is $\lambda = 0.68 \mu\text{m}$, the source size is $S = 300 \mu\text{m}$, the period of the gratings is $p_1 = p_2 = 20 \mu\text{m}$, and $z_0 = 5 \text{mm}$.

$$\begin{aligned}
\langle I(x_3) \rangle \propto & \sum_{n,n',m,m'=-\infty}^{\infty} a_n a_n^* b_m b_m^* \exp i x_3 [(n' - n) q_1 \\
& + (m' - m) q_2] \exp \left[-i (m + m') (n - n') \frac{q_1 q_2}{2k} z_1 \right] \\
& \times \delta[(n - n') q_1 z_{12} + (m - m') q_2 z_2],
\end{aligned} \quad (13)$$

which is equivalent to that obtained by Swanson and Leith [12].

However, when roughness is present, the width of the pseudo-images decreases, thus reducing the tolerances of optical devices based in generalized grating imaging systems. To analyze this effect, it is interesting to perform the following change of variables in (12): $N = n - n'$, $M = m - m'$, $u = n - N/2$, and $v = m - M/2$. As a result, the mean intensity is

$$\begin{aligned}
\langle I(x_3, z_2) \rangle \propto & \sum_{N,M=-\infty}^{\infty} \exp \left\{ - \frac{i x_3}{z_T} [N q_1 z_0 + M q_2 z_{01}] \right\} \\
& \times \operatorname{sinc} \left\{ \frac{S}{2 z_T} [N q_1 z_{12} + M q_2 z_2] \right\} \\
& \times \exp \left(- \left\{ \frac{z_0}{k T_0 z_T} [N q_1 z_{12} + M q_2 z_2] \right\}^2 \right) \\
& \times \sum_{u,v=-\infty}^{\infty} a_{u+N/2} a_{u-N/2}^* b_{v+M/2} b_{v-M/2}^* \exp \{ 2\pi i [u(N\gamma_{11} + M\gamma_{12}) \\
& + v(M\gamma_{22} + N\gamma_{12})] \},
\end{aligned} \quad (14)$$

where $\gamma_{11} = z_0 z_{12} / z_i z_T$, $\gamma_{22} = z_2 z_{01} R^2 / z_i z_T$, $\gamma_{12} = z_0 z_2 R / z_i z_T$, $R = p_1 / p_2$, and $z_i = p_1^2 / \lambda$. A given pseudoimage (N, M) presents a maximum value when the argument of the sinc function in Eq. (14) is zero, resulting

$$z_2 = \frac{1}{RQ - 1} z_1, \quad (15)$$

where $Q = -M/N$. At the exact locations of the pseudoimages, the sinc term and the Gaussian term are unity and the intensity does not depend on the roughness parameters.

For the usual distances (millimeters–centimeters), pseudoimages are quite narrow and they do not overlap (pseudoimage isolation, regime 3 of Ref. [23]). The sinc term and the Gaussian term control the width of the pseudoimage, being both terms competitive. We will define the width of a given pseudoimage as

$$\omega_{N,M}^2 = \frac{\int (z_1 - \bar{z})^2 \langle \text{Amp}(z_2) \rangle dz_1}{\int \langle \text{Amp}(z_2) \rangle dz_1}, \quad (16)$$

where $\langle \text{Amp}(z_2) \rangle = \max \langle I_{N,M}(x_3, z_2) \rangle - \min \langle I_{N,M}(x_3, z_2) \rangle$ and $\bar{z} = \int z_1 \langle \text{Amp}(z_2) \rangle dz_1 / \int \langle \text{Amp}(z_2) \rangle dz_1$. The width of a given pseudoimage (N, M) is dependent on the correlation length of roughness T_0 , as it is shown in Fig. 4.

For low values of T_0 , the Gaussian term controls the width of the pseudoimage which increases linearly as

$$\omega_{N,M} \approx \frac{kT_0 z_T}{\sqrt{2} z_0 N q_1} \quad (17)$$

However, when roughness is very low, the width of the pseudoimage is controlled by the sinc function, resulting in

$$\omega_{N,M} \approx \frac{2.6 z_T}{SN q_1} \quad (18)$$

This effect can be observed in Fig. 4a. For low values of T_0 , the width of the pseudoimage presents a linear dependence with T_0 . On the other hand, when T_0 is large, then the width is constant. We can also see in Fig. 4b that, depending on the value of T_0 , the shape of the pseudoimage varies from a Gaussian shape for low values of T_0 up to a maximum with several lobes when roughness is null.

3. Conclusions

In this work, we have performed an analysis of the behavior of a double grating system with a steel tape grating. Moiré configuration has been shown to strongly depend on the roughness of the grating and the self-imaging process eventually disappears as the distance between the two diffraction gratings increases. On the contrary, for the Lau and Generalized grating imaging configurations, the roughness of the steel tape grating does not affect the self-imaging process, although it affects the depth of focus of the self-images.

Acknowledgements

The authors thank Agustin Gonzalez-Cano for his invaluable help. This work was supported by the DPI2005-02860 project of the Ministerio de Educación y Ciencia of Spain and the “Tecnologías avanzadas para los equipos y procesos de fabricación de 2015: e-eficiente, e-cológica, e-máquina” CENIT project of the Ministerio de Industria, Turismo y Comercio. During the realization of this work Sanchez-Brea was contracted by the Universidad Complutense de Madrid under the “Ramón y Cajal” research program of the Ministerio de Educación y Ciencia of Spain.

References

- [1] G.W.R. Leibbrandt, G. Harbers, P.J. Kunst, *App. Opt.* 35 (1996) 6151.
- [2] Y. Xu, O. Sasaki, T. Suzuki, *Opt. Lett.* 28 (2003) 1751.
- [3] Y. Xu, O. Sasaki, T. Suzuki, *App. Opt.* 43 (2004).
- [4] I.B. Gornushkin, N. Omenetto, B.W. Smith, J.D. Winefordner, *App. Spectrosc.* 58 (2004).
- [5] S. Grabarnik, R. Wolffenbuttel, A. Emadi, M. Loktev, E. Sokolova, G. Vdovin, *Opt. Express* 15 (2007) 3581.
- [6] K. Patorski, The self-imaging phenomenon and its applications, in: E. Wolf (Ed.), *Progress in Optics* 27, North Holland, Amsterdam, 1989.
- [7] A.W. Lohmann, D.E. Silva, *Opt. Commun.* 2 (1971) 413.
- [8] K. Patorski, *Moiré Metrology*, Pergamon, New York, 1998.
- [9] E. Lau, *Ann. Phys.* 6 (1948) 417.
- [10] D. Crespo, J. Alonso, T. Morlanes, E. Bernabéu, *Opt. Eng.* 39 (2000) 817.
- [11] J. Jahns, W. Lohmann, *Opt. Commun.* 28 (1979) 263.

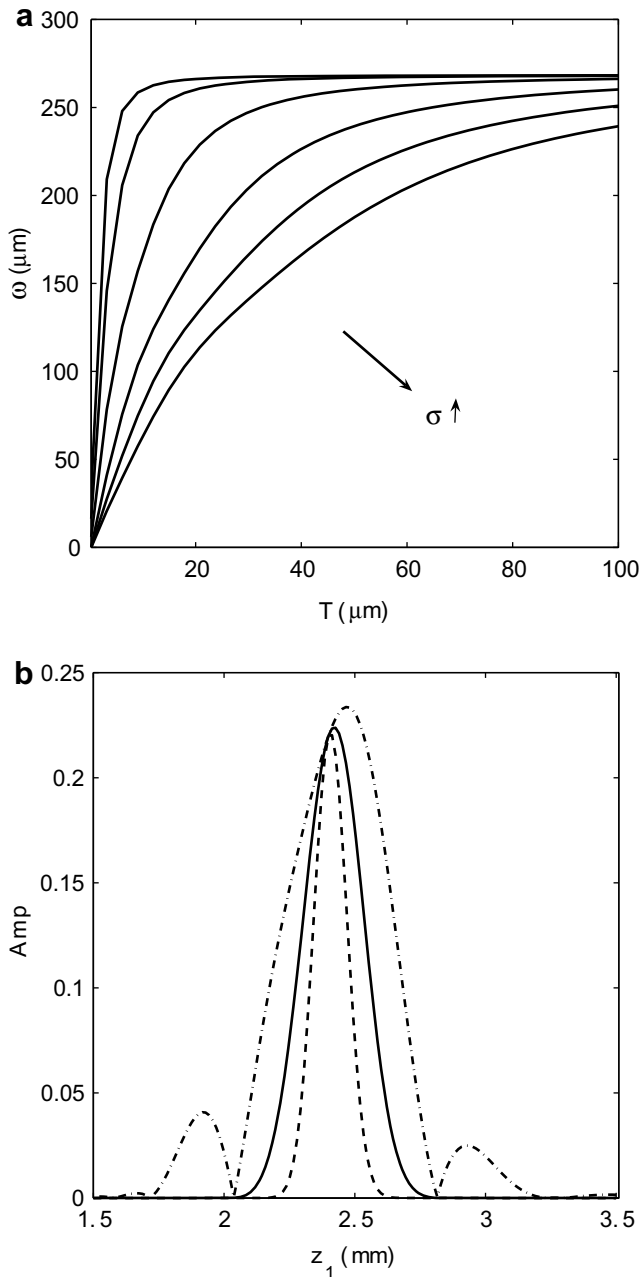


Fig. 4. (a) Width of the pseudoimage $(1, -2)$ at $z_2 = 2.4$ mm, defined as Eq. (16), for different values of σ : $0.05 \mu\text{m}$, $0.1 \mu\text{m}$, $0.25 \mu\text{m}$, $0.5 \mu\text{m}$, $0.75 \mu\text{m}$, and $1 \mu\text{m}$. The wavelength is $\lambda = 0.68 \mu\text{m}$, the source size is $S = 300 \mu\text{m}$, the period of the gratings is $p_1 = p_2 = 20 \mu\text{m}$, and $z_1 = 5$ mm. (b) Profile of the pseudoimage $(1, -2)$ for different values of the correlation length T_0 for the same conditions of (a) when $T_0 = 5 \mu\text{m}$ (dashed), $T_0 = 10 \mu\text{m}$ (solid), and $T_0 = 50 \mu\text{m}$ (dashed-dot).

- [12] G.J. Swanson, E.N. Leith, *J. Opt. Soc. Am. A* 2 (1985) 789.
- [13] S.C. Som, A. Satpathi, *J. Mod. Opt.* 37 (1990) 1215.
- [14] D. Crespo, J. Alonso, E. Bernabeu, *J. Opt. Soc. Am. A* 17 (2000) 1231.
- [15] D. Crespo, J. Alonso, E. Bernabeu, *Appl. Opt.* 41 (7) (2002) 1223.
- [16] Fagor Automation S. Coop. (www.fagorautomation.com), Heidenhain Cooperation (www.heidenhain.com), Renishaw Group (www.renishaw.com).
- [17] F.J. Torcal-Milla, L.M. Sanchez-Brea, E. Bernabeu, *Appl. Opt.* 46 (2007) 3668.
- [18] L.M. Sanchez-Brea, F.J. Torcal-Milla, E. Bernabeu, *J. Opt. Soc. Am. A* 25 (2008) 828.
- [19] P. Beckmann, *The Scattering of Electromagnetic Waves from Rough Surfaces*, Artech House INC, 1987.
- [20] J.A. Ogilvy, *Theory of Wave Scattering from Random Rough Surfaces*, IOP, Bristol, 1991.
- [21] F. Perez-Quintán, A. Lutenberg, M.A. Rebollo, *Appl. Opt.* 45 (2006) 4821.
- [22] G.J. Swanson, E.N. Leith, *J. Opt. Soc. Am. A* 72 (1972) 552.
- [23] L. Garcia-Rodriguez, J. Alonso, E. Bernabeu, *Opt. Express* 12 (2004) 2529.